Journal of Fluorescence (2019) 29:137–144
https://doi.org/10.1007/s10895-018-2321-5

ORIGINAL ARTICLE

N- and O-Doped Carbon Dots for Rapid and High-Throughput Dual Detection of Trace Amounts of Iron in Water and Organic Phases

Yuan He[1] · Zhenzhen Feng[2] · Xinjian Shi[3] · Shan Li[3] · Yunguo Liu[1] · Guangming Zeng[1] · Hua He[3]

Received: 11 September 2018 / Accepted: 22 October 2018 / Published online: 7 November 2018

Abstract

In this work, we report a dual use of highly fluorescent N- and O-doped carbon dots (CDs) for rapid and high-throughput trace analysis of iron in water and organic phases. The CDs are rapidly synthesized in a sealed vessel via microwave irradiation within 5 min, and they exhibit high quantum yields of 80% with sensitive quenching responses to iron contents. Combined with a microplate fluorescence reader, a rapid and high-throughput assay for ions is further developed. The whole process from the CD synthesis to the detection output can be accomplished within 15 min. The limits of detection for Fe^{3+} in aqueous solution and ferrocene in organic gasoline are determined down to 0.05 mM. Furthermore, this method has been successfully used to determine the level of irons in real gasoline for quality evaluation. The results have an excellent agreement with atomic absorption spectrophotometric measurements. The CD-based facile assay with lower cost, use of less sample, and higher-throughput holds great promise as a powerful tool for iron detection in water and organic phase samples.

Keywords Carbon dots · Fluorescence · Dual use · Iron detection · High throughput

Introduction

Fluorescent carbon nanoparticles, also known as carbon dots (CDs), have recently attracted great attentions for a range of wide applications such as biosensors, bioimaging, optoelectronics, photocatalysis due to their easy fabrication, low-cost and good biocompatibility [1–5]. Among those applications, fluorescent detection of metal ions is representing one of the most promising applications [6]. Owing to carbon-based nanostructure and versatile surface groups, CDs exhibit intense fluorescence with dramatic quenching or enhancement toward specific metal ions, which is substantially exploited for ion detection [7–11]. To achieve a sensitive detection to metal ions, highly fluorescent CDs with chemical structures specifically responding to metal ions are indispensable, but the availability of such CDs depends on their synthetic routes. Currently, the synthesis of CDs is divided into two major strategies, i.e., "top-down" and "bottom-up" routes. The former consists of acid-assisted cutting from different carbon sources (e.g. carbon black, carbon fiber, graphite or graphene) with H_2SO_4/HNO_3 over several hours to several days [12–14]. The fluorescence quantum yields (QYs) of the resultant CDs are generally lower than 10%. The latter produces CDs based on the dehydration and carbonization of small molecules or carbohydrate compounds, such as citric acid, arginine, glucose and polyethylene glycol (PEG) with hydrothermal treatments [15–20]. Such routes allow preparing highly fluorescent CDs (QYs ≥ 30%) as well as facilitating incorporation of other elements including N, S and P into the products [21–24]. The resultant versatile groups or surface structures on the CDs afford well for sensitive and specific response to different metal ions.

Of those metal ions, the detection of iron ions has become an exciting research field in recent years owing to their versatile existence in biological system,

✉ Yunguo Liu
liuyunguo@hnu.edu.cn

✉ Hua He
huahe@upc.edu.cn

[1] College of Environmental Science and Engineering, Hunan University, Changsha 410082, People's Republic of China

[2] Testing Institute for Chemicals & Minerals, Shandong Entry-Exit Inspection and Quarantine Bureau, 99 Huanghe East Road, Huangdao District, 266500 Qingdao, People's Republic of China

[3] State Key Laboratory of Heavy Oil Processing and College of Chemical Engineering, China University of Petroleum (East China), 66 Changjiang West Road, Huangdao District, Qingdao 266580, People's Republic of China

environment, and industry products. For example, Fe^{3+} ion is biologically important and plays key roles in oxygen uptake and oxygen metabolism [25]. The deficiency of Fe^{3+} leads to anemia while the excess of iron in the body causes liver and kidney damage [26]. In addition to the detection of aqueous iron ions, the determination of iron in organic phase is widespread in practical demand such as industrial products and organic-involved environmental system. For instance, ferrocene and its derivatives are key antiknock agents used in the fuel, and they were previously added into the gasoline to improve the octane number [27–29], but has been banned now for the possible cause of wear and tear to the engine with a strict limit of less than 0.01 g/L iron contents. The determination of irons thus becomes a commonly requested procedure to qualify the gasoline quality. In addition, benefiting from the unique fluorescent and chemical properties, CDs have been explored for iron ion detection, but they are mainly focused on the aqueous system [21, 30]. In recent years, although organic-soluble CDs have been synthesized for their applications in organic phase [31–34], no evidences show that such CDs can exhibit fluorescence quenching toward iron contents. Thus far, the use of CDs for iron detection in aqueous and organic phase is still lacking. Herein, we report a dual use of highly fluorescent CDs for iron detection in water and organic phases. The CDs are rapidly prepared via microwave irradiation within 5 min, and demonstrated to be N- and O-doped carbon nanostructure. Because of the sensitive quenching response to iron in aqueous and organic solution, the CDs can be explored to detect iron contents in two phases. Furthermore, in order to achieve low-cost and time-saving detection, a high-throughput assay of iron is developed with the limits of detection (LOD) down to 0.05 mM. The whole process from the CD synthesis to the result output is only required within 15 min. Finally, this method has been used to evaluate the gasoline quality by determining the level of irons.

Experimental

Materials and Reagents

Citric acid (CA) was purchased from Sigma-Aldrich Chemical Co. (St. Louis, MO, USA). Ethylenediamine (EDA, ≥ 99.0%), ethanol (≥ 99.7%), ferrocene (≥ 98%), and metal chlorides of ≥98% purity ($FeCl_3$, $FeCl_2$ NaCl, KCl, NH_4Cl, $MgCl_2$, $ZnCl_2$, $MnCl_2$, $CaCl_2$, $BaCl_2$, and $CuCl_2$) were purchased from Sinopharm Chemical Reagent Co. (China). Gasoline was provided by Testing Institute for Chemicals & Minerals, Shandong Entry-Exit Inspection and Quarantine Bureau, China. Ultra-pure water (18.2 MΩ) was prepared by a Milli-Q Millipore system. All reagents were used as received without any further purification.

Synthesis and Characterization of CDs

1.4 g CA and 1.8 mL EDA were dissolved in 30 mL ultra-pure water. The solution was transferred to a sealed digestion vessel in the microwave digestion furnace. The microwave digestion system (WX-4000, Shanghai Yi-Yao Instruments) was equipped with controllable temperature units within variation of ±1 °C at the set temperature. When set at 600 W power, the reaction temperature was rapidly elevated to 200 °C. The CD synthesis process could be completed within 5 min. The CD samples were diluted for optical characterizations. Ultraviolet-visible (UV-Vis) absorption spectra were obtained using a Shimadzu UV-2450 spectrophotometer. Fluorescence spectra and excitation-emission matrix were recorded by the Horiba FluoroMax-4 spectrometer. All optical measurements were performed at room temperature under ambient conditions. The QY of CDs was determined using quinine sulfate in 0.1 M H_2SO_4 aqueous solution (QY = 54%) as a reference standard as described previously [16, 35]. Briefly, the absorbance for the standard and CD samples at the excitation wavelengths and the fluorescence spectra of the same solutions were measured, respectively. Six different concentrations of quinine sulfate and CD aqueous solutions (absorbance at excitation wavelength < 0.1) were used in the measurements. The integrated fluorescence intensity against absorbance was plotted. The plot should be a straight line with a gradient M, which was used to calculate the QY according to the following equation

$$\varphi_x = \varphi_s \left(\frac{M_x}{M_s}\right)\left(\frac{\eta_x}{\eta_s}\right)^2$$

where the subscripts s and x denote standard and test samples, respectively, ϕ is QY, and η is the refractive index of the solvent. The excitation wavelength for measurements of QY was set at 350 nm in our experiments. TEM samples were prepared by dropping the CD solution onto carbon-coated copper grids with excess solvent evaporated. TEM images were recorded on a JEM-2100 electron microscope operating at 200 kV. Powder X-ray diffraction (XRD) pattern was obtained using an automated diffractometer (X'Pert PRO MPD, Philips, Eindhoven, Netherlands) with Cu Kα1 radiation. Fourier transform infrared (FTIR) spectra were recorded by a NICOLET 6700 IR spectrometer (Thermo Scientific). X-ray photoelectron spectroscopy (XPS) measurements were carried out on a VG-Scientific ESCALAB 250 spectrometer with a monochromatic Al Kα X-ray source at 1486.6 eV. ^1H and ^{13}C nuclear magnetic resonance (NMR) spectra were recorded on a Bruker Avance III 600 MHz spectrometer.

Fluorescence Detection and Data Analysis

In a typical test, 100 μL of CD aqueous solution (the absorbance at 350 nm was measured to be 0.2) was put into each well in a 96-well microplate. Then, 100 uL of the aqueous solution with iron ions or other metal ions (Na^+, K^+, NH_4^+, Mg^{2+}, Zn^{2+}, Mn^{2+}, Ca^{2+}, Ba^{2+} and Cu^{2+}) was added into each well. The 96-well microplate was loaded into a microplate autoreader (Molecular Devices, M2e) for fluorescence measurements. The excitation wavelength was set at 350 nm. The obtained data array is processed with a custom-made MATLAB software into the image show and the readout of detection results. The LOD was defined as the analyte concentration that generates a signal quenching lower than the mean value minus three times the standard deviations of the blank samples without the analytes.

Results and Discussion

Morphology and Optical Properties

The CDs were prepared based on the condensation and carbonization of CA and EDA. Upon microwave irradiation, the solution temperature was rapidly elevated above 200 °C, allowing CDs to be produced within 5 min on a large scale. Figure 1a shows a transmission electron microscopy (TEM) image of the resultant CDs. The uniform dispersion was clearly observed as shown in the histogram (Fig. 1b). The particle size was determined to be about 3.2 ± 0.56 nm. The XRD pattern of CDs shows a broad diffraction peak centered at $2\theta = 24^o$ ($d_{002} = 0.34$ nm) (Fig. 1c), which is attributed to turbostratic carbon phase [36]. The excitation-emission matrix shows that the CDs have strong fluorescence emission ranging from 400 nm to 500 nm (Fig. 2a). The optimal excitation wavelength is centred at about 350 nm. The intense fluorescence could also be directly observed under UV lamp as shown in the inset. In line with the optimal excitation, the UV-vis spectrum of the CDs shows a peak at around 350 nm, which was attributable to n-π* transition of C=O (Fig. 2b). Besides, another absorption peak at 238 nm was observed, indicating π–π* transition of C=C. This suggested the condensation of the molecular precursors and the formation of CDs. Figure 2c shows a typical fluorescence spectrum of the CDs at the excitation of 350 nm. The narrow and symmetric shape is clearly peaked at 440 nm. The fluorescence quantum yield (QY) was measured to be 80% with quinine sulfate as a reference standard. Upon the addition of Fe^{3+} into the solution, however, the fluorescence is quenched with a dramatic decrease in intensity. The sensitive response implies that the CDs can be developed as a promising sensor for detection of Fe^{3+}.

Surface Characterizations

In order to exploit the use of CDs as an effective ion sensor, we try to probe the quenching origin of fluorescent CDs by performing full characterizations. As the synthetic precursors, a CA molecule has three carboxyl groups while an EDA molecule has two amine groups. Although the synthetic reaction was conducted at a CA/EDA molar ratio of 1 to 3, the resultant CDs were negatively charged, as established with the polyacrylamide gel electrophoresis (PAGE). Under the electric field, the CDs moved toward the anion electrode (Fig. 3a). This suggests the existence of carboxyl and/or hydroxyl groups on the particle surface. To verify the chemical structure of CDs, ^{13}C NMR and ^{1}H NMR measurements were performed. In the ^{13}C NMR spectrum (Fig. 3b), signals from 20 ppm to 100 ppm correspond to aliphatic (sp3) carbon atoms, and signals in the range of 100–185 ppm indicate sp2 carbon atoms. The peaks between 170 and 185 ppm are ascribed to carboxyl groups. In the ^{1}H NMR spectrum (Fig. 3c), the regions of 1–3 ppm for sp3 C-H protons, 3–4 ppm for the protons of hydroxyethyl adjacent to the amide bond and the hydroxyl group, and 5.5–8.5 ppm for the aromatic protons are observed. In addition, the FTIR spectrum demonstrates the presence of –COOH, C=O, C=N, C=C, and O-H (Fig. 3d). Both pure CA and CDs have vibrational absorption bands of O-H and C=O at 3100–3500 cm^{-1} and 1700–1750 cm^{-1}, respectively. For CDs, the peaks at 1640 and 1325 cm-1 are

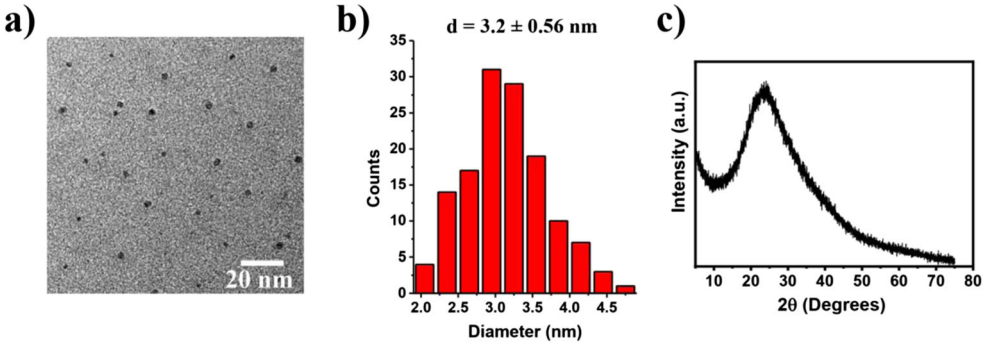

Fig. 1 Morphology and structure of CDs. **a** TEM image, **b** the particle size distribution determined from TEM images, and **c** XRD spectrum

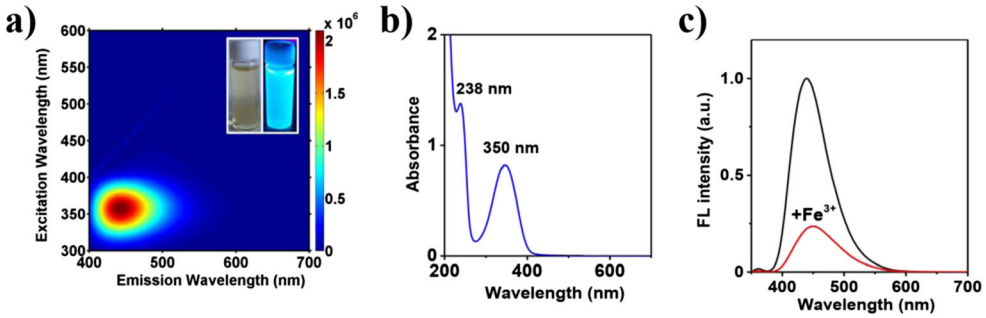

Fig. 2 Optical properties of CDs. **a** The excitation-emission matrix. Insets show the photographs of CD solution under daylight (Left) and 365 nm UV excitation (Right), **b** UV-vis absorption spectrum, and **c** fluorescence emission spectra of the CDs before and after the addition of Fe^{3+} ions (0.02 M)

attributed to the vibrational absorption band of C=O and C-O bonds, respectively. The broad absorption band emerged at 1530–1600 cm^{-1} are indicative of C=N/C=C stretching vibrations. The XPS of CDs further demonstrates the presence of C, N and O in the nanostructure (Fig. 4). The C1s spectrum indicates that CDs contains C=C (284.56 eV), C-N (285.7 eV) and C=N/C=O (287.47 eV) bonds. The N1 s spectrum reveals the existence of C-N (398.5 eV) and C=N (400.3 eV), while the O1s spectrum exhibits two peaks corresponding to C=O (530.75 eV) and C-O (531.6 eV). All these results suggest that the CDs are N- and O-doped aromatic-containing nanoparticles with –COOH and –OH groups on the surface. As has been previously demonstrated, phenolic hydroxyl groups can form a complex with iron ions where the electron transfer happens [37]. Thus, it is reasonably concluded that the phenolic hydroxyl-enriched CDs would coordinate with iron ions, facilitating charge transfer and leading to fluorescence quenching.

High-Throughput Assay of Iron Ions in Aqueous Solution

Although the CDs derived from CA and EDA has been recently reported for iron ion detection [30], the synthetic time was about 10 h. Furthermore, the detection method for metal ions was based on the measurement of fluorescence spectra of CDs and their intensity changes in response to analytes. This method is time-consuming and labour-intensive because of the lack of high-throughput capability [21, 30]. When analysing mass samples, e.g. in screening detection for practical industry products, a rapid and facile high-throughput assay is quite in demand for an analyst. To exploit CD-based

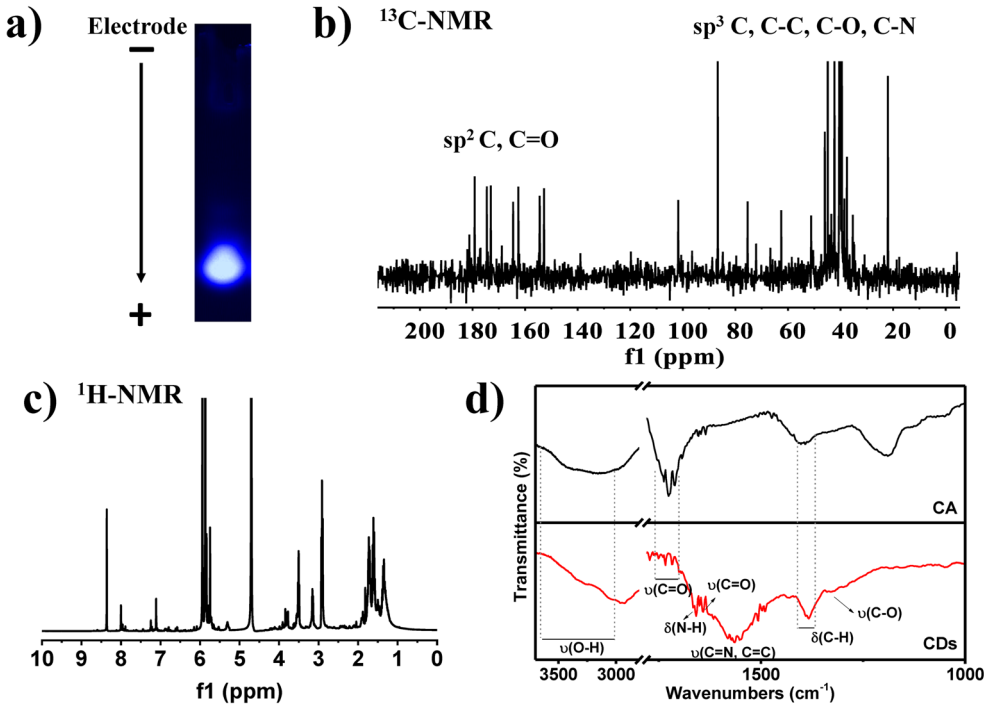

Fig. 3 Surface characterizations of CDs. **a** PAGE analysis, **b** ^{13}C-NMR spectrum, **c** ^{1}H-NMR spectrum, and **d** FTIR spectra

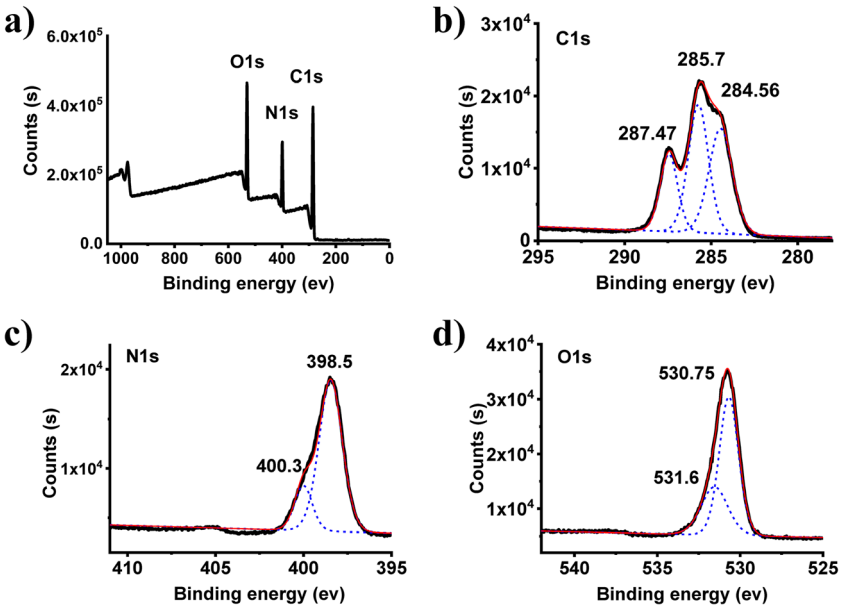

Fig. 4 (a) XPS spectra of CDs; (b) deconvoluted C 1 s spectrum of CDs; (c) deconvoluted N 1 s spectrum of CDs; (d) deconvoluted O 1 s spectrum of CDs

fluorescence detection for practical applications, we use a microplate reader with a 96-well microplate for fluorescence measurements (Fig. 5a). The microplate allows high-throughput detection of mass samples as well as measuring duplicate samples for averaged intensity to minimize experimental errors. The obtained array data was automatically processed with a custom-made MATLAB software into the image show and readout of detection results (Fig. 5b–e). The process from the sample processing to the readout was taken in less than 10 min. Figure 5b shows a color-coded heat-map image of the array data from CD solutions in the presence of different metal ions. In the image, every pixel represents the fluorescence value of a well averaged from three repeated measurements. For each solution sample, four duplicate wells were used, which created 2 × 2 pixel^2 in the image. As can be seen, the image shows a significant brightness difference in response to various metal ions at the same concentration. For those wells in the presence of Fe^{3+} and Fe^{2+}, the fluorescence signals are weak. Especially in the case of Fe^{3+}, the fluorescence intensity decreases down closely to zero. The quantitative outputs for each sample are plotted with the mean value ± standard deviation in Fig. 5c. High specificity of the CDs toward Fe^{3+} is clearly demonstrated. Figure 5d shows a color-coded heat-map image of the array data from a series of CD solutions with Fe^{3+} concentration grades. The gradual changes in color indicate the Fe^{3+} concentration-dependent fluorescence of CDs. The quantitative outputs shown in Fig. 5e present a good linearity ranging from 0.1 mM and 1 M with a correlation coefficient of 98.3%. The limit of detection (LOD) for Fe^{3+} was determined to about 0.05 mM. In addition, the same measurement and analysis for Fe^{2+} was performed. As shown in Fig. 5f, the fluorescence of CDs also displays a good linear response against Fe^{2+} concentration with a LOD down to about 0.2 mM.

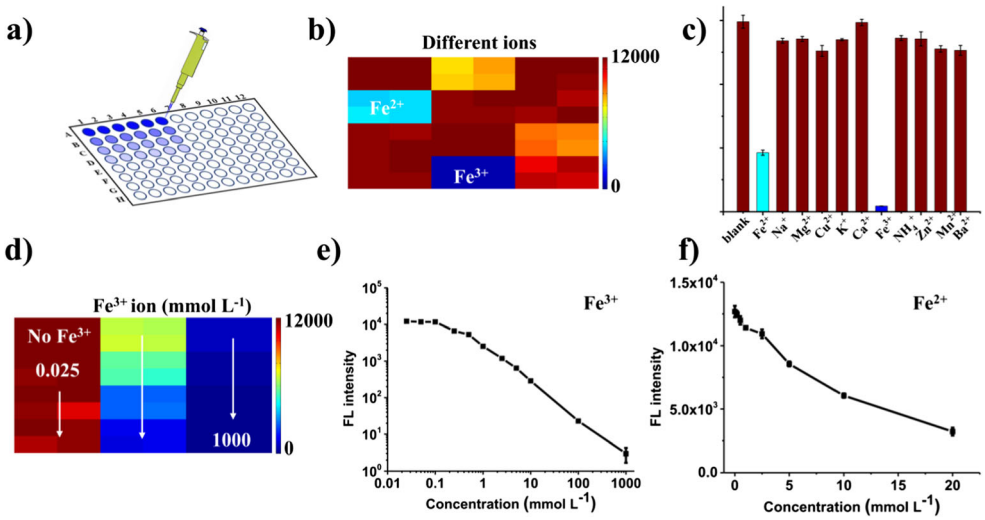

Fig. 5 The detection of iron ions in aqueous solution. **a** scheme of high-throughput detection, **b** fluorescence heat map of CDs in the presence of different metal ions, **c** fluorescence intensity analysis of CDs against different metal ions, **d** fluorescence heat map of CDs in the presence of different concentrations of Fe^{3+}, **e** the fluorescence intensity vs Fe^{3+} concentration plot, and **f** the fluorescence intensity vs Fe^{2+} concentration plot

High-Throughput Assay of Irons in Gasoline

So far, most reports on the CDs for metal detection have been focused on their use in aqueous solution. However, the detection of metal contents in organic phase is in demand. For instance, ferrocene is a key Fe-based additive in the gasoline and fuel for improving their octane number, but the excessive addition was restricted by the governments (≤ 0.2 mM). The typical method for ferrocene determination is atomic absorption spectrometry (AAS). To extend the application range of CDs, we attempt to use CDs to detect ferrocene in gasoline. Nevertheless, owing to its strong polarity, CDs can hardly be dispersed in gasoline. To improve the solubility of CDs, we tested many polar solvents and ultimately chose ethanol as a co-solvent for CDs in gasoline. As shown in Fig. 6a, the CDs exhibit uniform and bright fluorescence in gasoline with the help of 30% ethanol. Furthermore, it was found that the fluorescence of CDs had sensitive response to ferrocene in gasoline. The gasoline samples were then analysed with the high-throughput detection method we developed here. Figure 6b and c present the color-coded heat-map image of gasoline samples with different concentrations of ferrocene and the quantitative outputs for each sample, respectively. The good linearity is exhibited from 0.05 mM to 5 mM ferrocene with a LOD down to 0.05 mM. The high sensitivity allows one to evaluate the antiknock quality of gasoline by determining if its iron level falls within the threshold of 0.2 mM. Figure 6d shows the fluorescence intensity of CDs in two real gasoline samples. A significant fluorescence decrease in unquantified gasoline indicates that the CD-based quenching assay is a convenient tool for the quality evaluation of gasoline. To examine the accuracy of this assay, we finally compared the results with those measured by atomic absorption spectroscopy (Table 1). The good agreements with small relative errors were observed between two methods, yet the CD-based assay allows the measurements of irons to be achieved with higher-throughput, use of less sample and lower-cost instrumentation platform.

Table 1 Comparison of assay results from gasoline samples measured by CD-based and AAS methods

Sample no.	CD-based (mM)		AAS (mM)	Relative errors
	Mean value	RSD		
1	0.052	9.2%	0.048	8%
2	0.10	7.4%	0.095	5%
3	0.30	8.1%	0.28	7%
4	0.51	6.7%	0.48	6%

The results are average values of twelve measurements

Conclusion

In conclusion, we have reported a dual use of highly fluorescent N- and O-doped CDs for iron detection in water and organic phases. The CDs were prepared within 5 min via microwave-assisted synthetic route. They exhibit high QYs up to 80% with sensitive and selective quenching responses to iron ions in aqueous solution and ferrocene in gasoline. The fluorescence detection was performed on a microplate reader, and then processed with a custom-made MATLAB software. It thus allows high-throughput

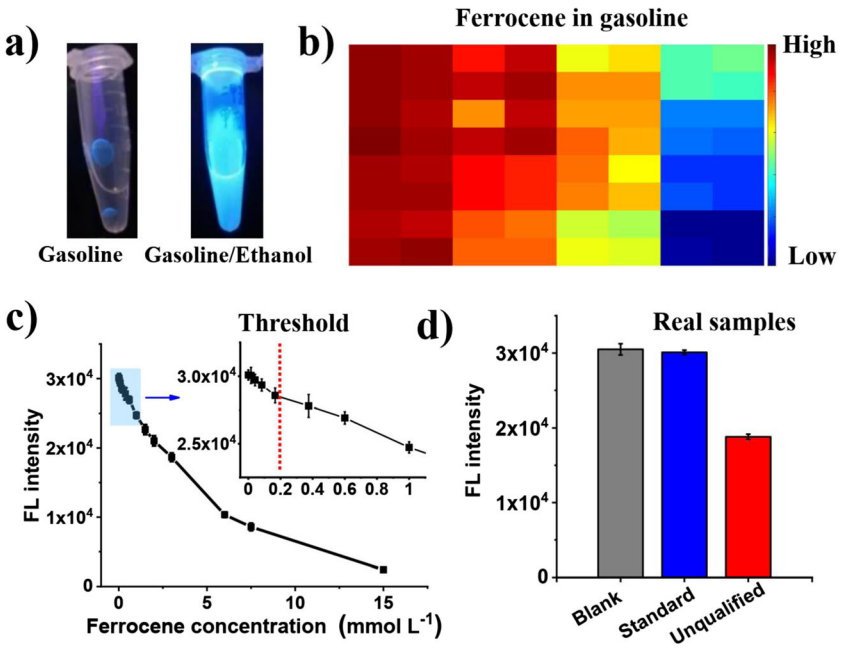

Fig. 6 The detection of irons in gasoline. **a** photographs of CDs in ethanol and gasoline containing 30% ethanol under 365 nm UV excitation. **b** fluorescence heat map of CDs in the presence of different concentrations of ferrocene. **c** the intensity vs ferrocene concentration plot. Inset shows the enlarged view of transparent blue region for clearer observation. **d** fluorescence intensity analysis of CDs in two real gasoline samples, standard vs unquantified gasoline

detection and rapid readout of the iron levels. The whole process from the CD synthesis to the result output can be completed within 15 min. Because of lower cost, use of less sample, and higher-throughput, this CD-based method can be used as a promising technique for iron detection in aqueous and organic environments.

Acknowledgments This work was supported by General Administration of Quality Supervision, Inspection and Quarantine of the People's Republic of China scientific research project (2017IK236), Shandong Exit&Entry Inspection and Quarantine Bureau Science and Technology Project (SK201642), and the Fundamental Research Funds for the Central Universities (18CX02126A).

References

1. Chen TH, Tseng WL (2017) Self-assembly of monodisperse carbon dots into high-brightness nanoaggregates for cellular uptake imaging and Iron (III) sensing. Anal Chem 89:11348–11356
2. Han C, Wang R, Wang K, Xu H, Sui M, Li J, Xu K (2016) Highly fluorescent carbon dots as selective and sensitive "on-off-on" probes for iron (III) ion and apoferritin detection and imaging in living cells. Biosens Bioelectron 83:229–236
3. Jiang K, Sun S, Zhang L, Lu Y, Wu A, Cai C, Lin H (2015) Red, green, and blue luminescence by carbon dots: full-color emission tuning and multicolor cellular imaging. Angew Chem Int Ed 54: 5360–5363
4. Baker SN, Baker GA (2010) Luminescent carbon nanodots: emergent nanolights. Angew Chem Int Ed 49:6726–6744
5. Arcudi F, Đorđević L, Prato M (2016) Synthesis, separation, and characterization of small and highly fluorescent nitrogen-doped carbon NanoDots. Angew Chem Int Ed 55:2107–2112
6. Guo Y, Zhang L, Zhang S, Yang Y, Chen X, Zhang M (2015) Fluorescent carbon nanoparticles for the fluorescent detection of metal ions. Biosens Bioelectron 63:61–71
7. Zhou L, Lin Y, Huang Z, Ren J, Qu X (2012) Carbon nanodots as fluorescence probes for rapid, sensitive, and label-free detection of Hg^{2+} and biothiols in complex matrices. Chem Commun 48:1147–1149
8. Lu W, Qin X, Liu S, Chang G, Zhang Y, Luo Y, Asiri AM, Al Youbi AO, Sun X (2012) Economical, green synthesis of fluorescent carbon nanoparticles and their use as probes for sensitive and selective detection of mercury (II) ions. Anal Chem 84:5351–5357
9. Liu J-M, L-p L, Wang XX, Lin SQ, Cai W-L, Zhang LH, Zheng ZY (2012) Highly selective and sensitive detection of Cu^{2+} with lysine enhancing bovine serum albumin modified-carbon dots fluorescent probe. Analyst 137:2637–2642
10. Lv P, Yao Y, Zhou H, Zhang J, Pang Z, Ao K, Cai Y, Wei Q (2017) Synthesis of novel nitrogen-doped carbon dots for highly selective detection of iron ion. Nanotechnology 28:165502
11. Wang N, Wang Y, Guo T, Yang T, Chen M, Wang J (2016) Green preparation of carbon dots with papaya as carbon source for effective fluorescent sensing of Iron (III) and Escherichia coli. Biosens Bioelectron 85:68–75
12. Liu H, Ye T, Mao C (2007) Fluorescent carbon nanoparticles derived from candle soot. Angew Chem Int Ed 46:6473–6475
13. Sun YP, Zhou B, Lin Y, Wang W, Fernando KA, Pathak P, Meziani MJ, Harruff BA, Wang X, Wang H, Luo PG, Yang H, Kose ME, Chen B, Veca LM, Xie SY (2006) Quantum-sized carbon dots for bright and colorful photoluminescence. J Am Chem Soc 128:7756–7757
14. Liu F, Jang MH, Ha HD, Kim JH, Cho YH, Seo TS (2013) Facile synthetic method for pristine graphene quantum dots and graphene oxide quantum dots: origin of blue and green luminescence. Adv Mater 25:3657–3662
15. Zhu S, Meng Q, Wang L, Zhang J, Song Y, Jin H, Zhang K, Sun H, Wang H, Yang B (2013) Highly photoluminescent carbon dots for multicolor patterning, sensors, and bioimaging. Angew Chem Int Ed 52:3953–3957
16. Zhai X, Zhang P, Liu C, Bai T, Li W, Dai L, Liu W (2012) Highly luminescent carbon nanodots by microwave-assisted pyrolysis. Chem Commun 48:7955–7957
17. Krysmann MJ, Kelarakis A, Dallas P, Giannelis EP (2012) Formation mechanism of carbogenic nanoparticles with dual photoluminescence emission. J Am Chem Soc 134:747–750
18. Jaiswal A, Ghosh SS, Chattopadhyay A (2012) One step synthesis of C-dots by microwave mediated caramelization of poly(ethylene glycol). Chem Commun 48:407–409
19. Yang ZC, Wang M, Yong AM, Wong SY, Zhang XH, Tan H, Chang AY, Li X, Wang J (2011) Intrinsically fluorescent carbon dots with tunable emission derived from hydrothermal treatment of glucose in the presence of monopotassium phosphate. Chem Commun 47: 11615–11617
20. Peng H, Travas-Sejdic J (2009) Simple aqueous solution route to luminescent carbogenic dots from carbohydrates. Chem Mater 21: 5563–5565
21. Xu Q, Pu P, Zhao J, Dong C, Gao C, Chen Y, Chen J, Liu Y, Zhou H (2015) Preparation of highly photoluminescent sulfur-doped carbon dots for Fe (III) detection. J Mater Chem A 3:542–546
22. Li L, Yu B, You T (2015) Nitrogen and sulfur co-doped carbon dots for highly selective and sensitive detection of Hg (II) ions. Biosens Bioelectron 74:263–269
23. Gupta A, Chaudhary A, Mehta P, Dwivedi C, Khan S, Verma NC, Nandi CK (2015) Nitrogen-doped, thiol-functionalized carbon dots for ultrasensitive Hg (II) detection. Chem Commun 51:10750–10753
24. Wang W, Li Y, Cheng L, Cao Z, Liu W (2014) Water-soluble and phosphorus-containing carbon dots with strong green fluorescence for cell labeling. J Mater Chem B 2:46–48
25. Lynch SR (1997) Interaction of iron with other nutrients. Nutr Rev 55:102–110
26. Aisen P, Wessling-Resnick M, Leibold EA (1999) Iron metabolism. Curr Opin Chem Biol 3:200–206
27. Schug K, Guttmann HJ, Preuss A, Schädlich K (1990) Effects of ferrocene as a gasoline additive on exhaust emissions and fuel consumption of catalyst equipped vehicles. Society of Automotive Engineers (SAE) Paper, 900154. https://doi.org/10.4271/900154
28. Demirbas A, Balubaid M, Basahel A, Ahmad W, Sheikh M (2015) Octane rating of gasoline and octane booster additives. Pet Sci Technol 33:1190–1197
29. Herrmann WA (2002) Ferrocene as a gasoline and fuel additive. In: Cornils B, Herrmann WA (eds) Applied homogeneous catalysis with organometallic compounds, 2nd edn. Wiley-VCH Verlag GmbH, Weinheim, pp 586–590
30. Devi S, Kaur A, Sarkar S, Vohra S, Tyagi S (2018) Synthesis and characterization of highly luminescent N-doped carbon quantum dots for metal ion sensing. Integr Ferroelectr 186:32–39
31. Zhao P, Zhu L (2018) Dispersibility of carbon dots in aqueous and/or organic solvents. Chem Commun 54:5401–5406
32. Pei X, Xiong D, Wang H, Gao S, Zhang X, Zhang S, Wang J (2018) Reversible phase transfer of carbon dots between an organic phase and aqueous solution triggered by CO2. Angew Chem Int Ed 57: 3687–3691
33. Gu J, Li X, Hu D, Liu Y, Zhang G, Jia X, Huang W, Xi K (2018) Green synthesis of amphiphilic carbon dots from organic solvents: application in fluorescent polymer composites and bio-imaging. RSC Adv 8:12556–12561

34. Wu M, Zhan J, Geng B, He P, Wu K, Wang L, Xu G, Li Z, Yin L, Pan D (2017) Scalable synthesis of organic-soluble carbon quantum dots: superior optical properties in solvents, solids, and LEDs. Nanoscale 9:13195–13202
35. Melhuish W (1961) Quantum efficiencies of fluorescence of organic substances: effect of solvent and concentration of the fluorescent solute1. J Phys Chem 65:229–235
36. Liu Y, Xiao N, Gong N, Wang H, Shi X, Gu W, Ye L (2014) One-step microwave-assisted polyol synthesis of green luminescent carbon dots as optical nanoprobes. Carbon 68:258–264
37. Wesp EF, Brode WR (1934) The absorption spectra of ferric compounds. I. The ferric chloride-phenol reaction. J Am Chem Soc 56: 1037–1042